Available online at www.sciencedirect.com
SCIENCE DIRECT®
Mechanics of Materials 37 (2005) 287–298
MECHANICS OF MATERIALS
www.elsevier.com/locate/mechmat

Very high strain-rate response of a NiTi shape-memory alloy

Sia Nemat-Nasser *, Jeom-Yong Choi, Wei-Guo Guo, Jon B. Isaacs

Department of Mechanical and Aerospace Engineering, Center of Excellence for Advanced Materials, University of California, San Diego, 9500 Gilman Drive, La Jolla, CA 92093-0416, USA

Received 1 January 2004

Abstract

The compressive response of a NiTi shape-memory alloy is investigated at high strain rates, using UCSD's modified split Hopkinson pressure bar and a mini-Hopkinson bar with specially designed striker bars. To obtain a constant strain rate during the formation of the stress-induced martensite phase in a Hopkinson test, a copper-tube pulse shaper of suitable dimensions or a stepped striker bar is employed, since without a pulse shaper or with a uniform striker bar, the strain rate of the sample will vary significantly as the material's microstructure changes from austenite to martensite, whereas with proper pulse shaping techniques a nearly constant strain rate can be achieved over a certain deformation range. At a very high strain rate, the yield stress and the stress-induced martensite formation process are significantly different from those at moderately high strain rates, suggesting that, correspondingly, different microstructural changes may be involved in the phase transition regime. The material's yield stress appears lower when measured in a mini-Hopkinson bar (with very small samples) as compared with that measured by a 1/2-in. Hopkinson bar (with relatively large samples), possibly due to the sample size that may produce different deformation mechanisms within the superelastic strain range. The transition stress from the austenite to the martensite phase shows strain-rate sensitivity. This may be explained by considering the interfacial motion of the formed martensite phase, based on the thermally activated and dislocation-drag models. There exists a certain critical strain-rate level, at which the transition stress for the stress-induced martensite formation equals the yield stress of the austenite phase. Therefore, the shape-memory alloy deforms by the formation of stress-induced martensites, accompanied by the yielding of the martensite phase at this critical strain rate, while the material deforms plastically by the dislocation-induced plastic slip at strain rates above this critical level.

Keywords: NiTi; Shape-memory alloy; Stress-induced martensite; Plastic behavior; Hopkinson bar; Yield stress; Strain-rate sensitivity of transition stress

* Corresponding author. Tel.: +1 858 534 4772/4914; fax: +1 858 534 2727.
E-mail address: sia@ucsd.edu (S. Nemat-Nasser).

0167-6636/$ - see front matter © 2004 Elsevier Ltd. All rights reserved.
doi:10.1016/j.mechmat.2004.03.007

1. Introduction

Shape-memory alloys are functional materials with a variety of applications (Otsuka and Wayman, 1998; Van Humbeeck, 1999, 2001). Their mechanical properties and their microstructural changes at various strain rates and temperatures have been of considerable interest. The static superelastic properties of shape-memory alloys have been extensively studied (Jacobus et al., 1996; Lin et al., 1996; Shaw and Kyriakides, 1997; Entemeyer et al., 2000). In quasi-static loading conditions, the transition stress for stress-induced martensite formation increases with an increase in the strain rate. In addition, in the stress-induced martensite formation regime, the work-hardening rate increases with the increasing strain rate, due to the latent heat of transformation and the heat of deformation (McCormick et al., 1993; Shaw and Kyriakides, 1995; Tobushi et al., 1999). Their dynamic properties, however, have not been fully explored, especially their strain-rate sensitivity and their high strain-rate microstructural changes, due to the difficulty in controlling the strain rate. Chen et al. (2001) and Nemat-Nasser et al. (in press) have used a pulse-shaping technique to control the strain rate within the stress-induced martensite formation regime in dynamic loading at moderately high strain rates. They point out that the stress for the stress-induced martensite formation increases with the increasing strain rate. Especially, it is reported that the strain-rate sensitivity of stress-induced martensite formation abruptly increases at strain rates exceeding 1000/s (Nemat-Nasser et al., in press). However, we are not aware of any study that addresses the plastic behavior of this material at very high strain rates, i.e., greater than 10,000/s.

Here, we report some recent experimental investigations of the dynamic plastic response of a NiTi shape-memory alloy over a range of high strain rates at 296 K initial temperature, using a recovery Hopkinson pressure bar system. To examine the stress-induced martensite formation at strain rates greater than 10,000/s, we have used a mini-Hopkinson bar system with stepped striker bars, in order to obtain relatively constant strain rates.

2. Experimental procedure

The composition of the material used in the present study is 50.4(at%)Ni–49.6(at%)Ti and its A_f temperature is 296 K. Circular cylindrical samples with 5 mm nominal diameter and 5 mm nominal length (for moderately high strain-rate tests) and 2 mm nominal diameter and 1.5 mm nominal length (for very high strain-rate tests) are cut by electro-discharge machining (EDM).

The dynamic compression tests are carried out using the UCSD's recovery Hopkinson technique with a pulse shaper (Nemat-Nasser et al., 1991; Nemat-Nasser and Isaacs, 1997) and the mini-Hopkinson bar with stepped striker bars, in order to obtain relatively constant strain rates at very high strain rates. Fig. 1 is a schematic diagram of the split Hopkinson pressure bar, showing a striker bar, a pulse-shaping material, an incident bar, and a transmission bar. The specimen is sandwiched between the incident and transmission bars. Both ends of the specimen are greased to reduce the end-friction effect on the specimen deformation during the dynamic test. Experimental techniques for pulse shaping in shape-memory alloy tests are discussed in detail by Nemat-Nasser et al. (in press).

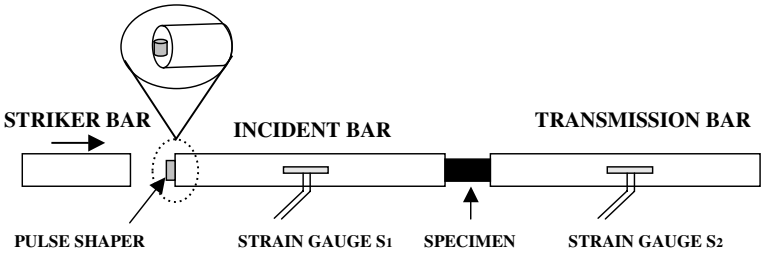

Fig. 1. Schematic diagram of the split Hopkinson bar with a pulse shaper.

To study the plastic response of the material, the strain must exceed 8%, above which a permanent plastic deformation occurs. The microstructure of the specimens that are plastically deformed in compression at high strain rates using 1/2-in. and mini-Hopkinson bars, is examined using TEM. Samples for TEM observations are cut with a low speed diamond saw, parallel to the compression axis. In the case of the 1/2-in. specimens, thin foils are prepared by grinding the cut sheets to about 150–100 μm and then they are electropolished using a twin-jet method in an electrolyte of acetic acid and perchloric acid, 9:1 volume, at 296 K. In the case of small mini-Hopkinson bar specimens, mechanical grinding is used to produce 150–100 μm foils, which are then dimple-grinded and glued to nickel grids. These glued discs are ion-milled until perforation. TEM observations are carried out on a Philips CM200 at 200 kV, using a side entry type double-tilt specimen holder.

3. Results and discussion

3.1. Plastic response of NiTi at moderately high strain rates

To investigate the stress–strain relation of NiTi shape-memory alloys beyond the superelastic regime, which is marked by a critical strain, ε_{cr}, Hopkinson tests with a pulse shaper are performed at 296 K initial temperature. A copper-tube pulse shaper is used to obtain relatively constant strain rates for deformations beyond ε_{cr} (Nemat-Nasser et al., in press). Fig. 2 compares typical stress and strain rate results as functions of the strain for tests without and with a pulse shaper. The stress–strain curves are similar, but the transition stress of stress-induced martensite formation, σ^{s}_{fr}, is greater for the test performed without a pulse shaper which produces a rather high initial strain rate. As is seen, without a pulse shaper, the net decrease in the strain rate within the entire deformation regime is about 3000/s. With a pulse shaper, on the other hand, the time-variation of the strain rate is significantly smaller, with a net decrease of about 500/s. The strain rate with a copper-tube pulse shaper is relatively constant over a broad range of strains, as compared with the strain rate obtained without a pulse shaper. Thus, it can be concluded that, with a proper choice of a pulse shaper, a relatively constant strain rate can be attained. Fig. 3 shows the effect of a copper-tube pulse shaper on the time-variation of the strain. Even though with a pulse shaper the overall strain rate is constant over a range of strains, it may be divided into two regions, based on the corresponding stress response of the material,

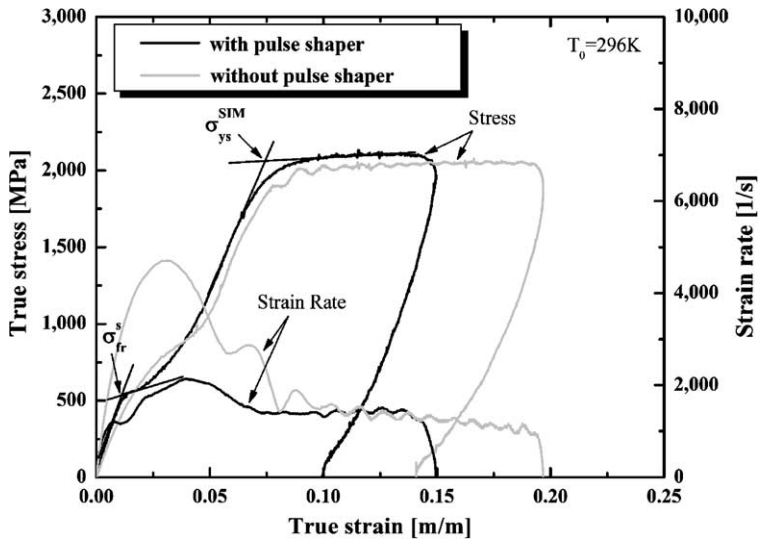

Fig. 2. Stress and strain rate as functions of strain, obtained using 1/2-in. Hopkinson bar with and without a pulse shaper.

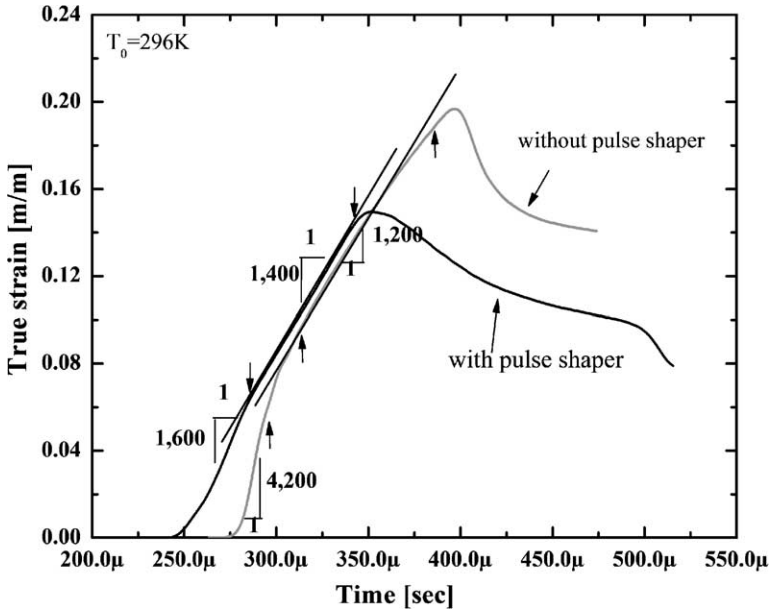

Fig. 3. Time-variation of strain for test using 1/2-in. Hopkinson bar with and without a pulse shaper.

i.e., a superelastic and a plastic one. As shown in Fig. 3, the strain rate without a pulse shaper consists of two distinctly different strain rates (slopes), but, with a pulse shaper, a more uniform strain rate is displayed. Two strain rate regimes, therefore, may be identified, depending on the mechanical response of the material: one during the stress-induced martensite formation, which corresponds to strains below approximately 0.06, and the other, a plastic deformation regime, which corresponds to strains above approximately 0.06. Without a pulse shaper, these strain rates are 4200 and 1200/s, while with a pulse shaper, they are 1600 and 1400/s, respectively.

Fig. 4 presents the variation of the stress as a function of the strain for indicated strain rates that are determined for strains within the range 0.06–0.2. As a comparison, a quasi-static stress–strain curve, obtained at a strain rate of 10^{-2}/s, is also included in Fig. 4. All stress–strain curves are similar beyond the critical strain, ε_{cr}. Roughly speaking, the transition stress for the stress-induced martensite formation depends on the strain rate, and the results in Fig. 4 provide evidence to support this. Moreover, the yield stress of the stress-induced martensite, σ_{ys}^{SIM}, measured at the intersection of the tangents to the ascending and the flat sections of the stress–strain curve, seems also to be dependent on the strain rate. The work-hardening rate within the plastic deformation region decreases with an increase in the strain rate from the quasi-static to the dynamic state. In the dynamic case, however, it is not very sensitive to the strain rate, based on the results obtained using a 1/2-in. Hopkinson bar.

3.2. Response of NiTi at very high strain rates

To attain strain rates greater than 10,000/s, we use very small samples in the UCSD's mini-Hopkinson bar system with uniform as well as stepped striker bars. Fig. 5 exhibits the variation of the stress and the strain rate as functions of the strain, obtained using uniform and stepped striker bars. The strain rate with a uniform striker bar initially increases and reaches approximately 20,000/s, then rapidly decreases before the yield point of the shape-memory alloy is reached. After yielding, the strain rate decreases at a roughly constant rate during the plastic deformation of the material. The

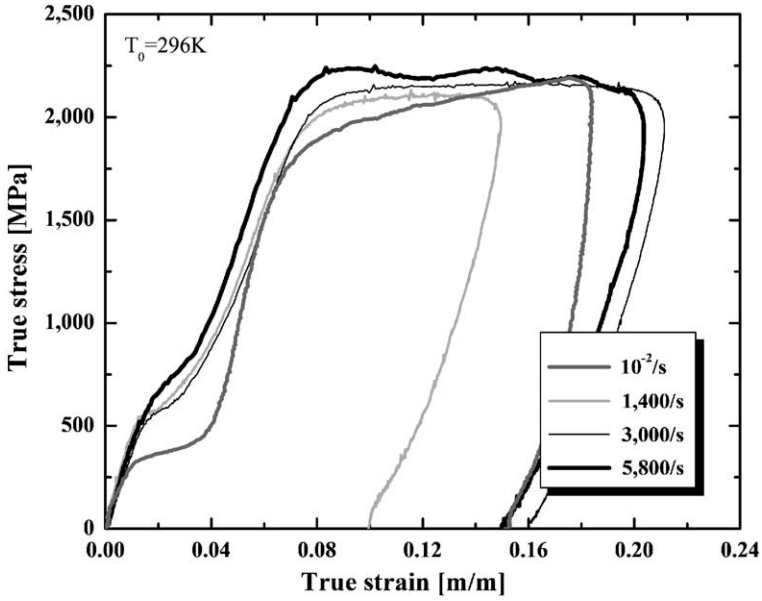

Fig. 4. Variation of stress with strain for tests using 1/2-in. Hopkinson bar with copper-tube pulse shapers at indicated strain rates.

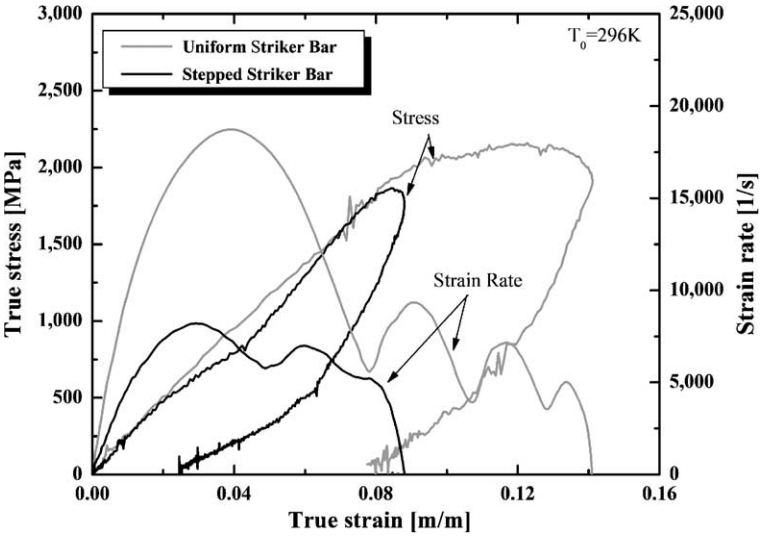

Fig. 5. Stress and strain rate as functions of strain obtained using mini-Hopkinson bar with a stepped striker bar and a uniform striker bar.

net decrease in the strain rate over the loading range is about 12,000/s. The stress–strain curve, however, is concave up until the plastic yielding begins, and then it is concave down. The shape of the stress–strain curve at strains below 0.08 is quite different than that in Fig. 4, which was obtained by the 1/2-in. Hopkinson bar. This is partly due to the different response of the material at different strain rates. Note that the initial elastic response of the austenite phase is expected to be

the same in all these tests, and the differences observed in Figs. 4 and 5 are due to the experimental errors, most likely due to the indentation of the mini-Hopkinson bar by the small samples.

To obtain relatively constant higher strain rates within the (as-expected) stress-induced martensite formation regime, we use a stepped striker bar. Even though the strain rate with stepped striker bar in Fig. 5, again initially increases and then decreases during the remaining deformation regime, the overall time-variation of the strain rate is significantly reduced, with a net decrease of about 3000/s, to roughly a constant value. For small strains, the stress–strain relation obtained using a stepped striker bar differs from that obtained using a uniform striker bar, as shown in Fig. 5, even if we consider the indentation effects. A transition point is observed in the stress–strain curve, obtained using a stepped striker bar, but there is no clear distinction between the stress-induced martensite formation regime and the transition stress. In addition, a superelastic response is displayed in the test with the stepped striker bar, even though the strain is not fully recovered at the instant of complete unloading.

Fig. 6 shows the variation of the stress as a function of the strain, obtained using a uniform striker bar. Comparing these results with those in Fig. 4, no clear transition stress for the stress-induced martensite formation is seen in these higher strain-rate tests, suggesting that a different material response may be involved in this phase transition regime. Within the plastic deformation regime, the flow stress of the material, tested in the mini-Hopkinson bar, is about 2 GPa, but that tested in the 1/2-in. Hopkinson bar is about 2.3 GPa, at comparable strain rates. This suggests that the material response within the strain range of the stress-induced martensite formation regime affects the flow stress in the plastic regime.

Fig. 7 shows typical graphs of the time-variation of the true strain. As seen, the strain rate with uniform striker bar has two distinct slopes with the average strain rate of 16,900/s below 0.08 strain and a strain rate of about 6500/s beyond 0.08 strain. However, the strain rate with the stepped striker bar, measured between the arrows, is about 6600/s, suggesting that a relatively constant strain rate has been attained at this rather high strain rate.

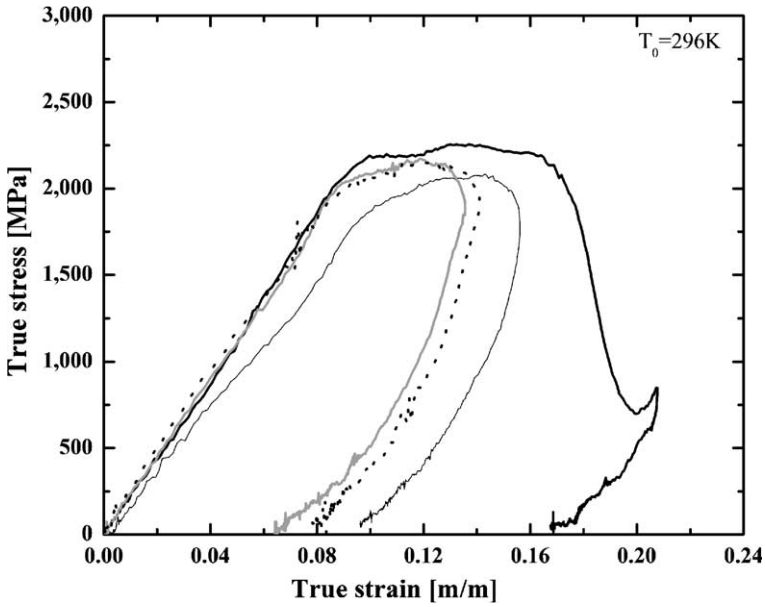

Fig. 6. Stress–strain curves obtained using the mini-Hopkinson bar with uniform striker bar.

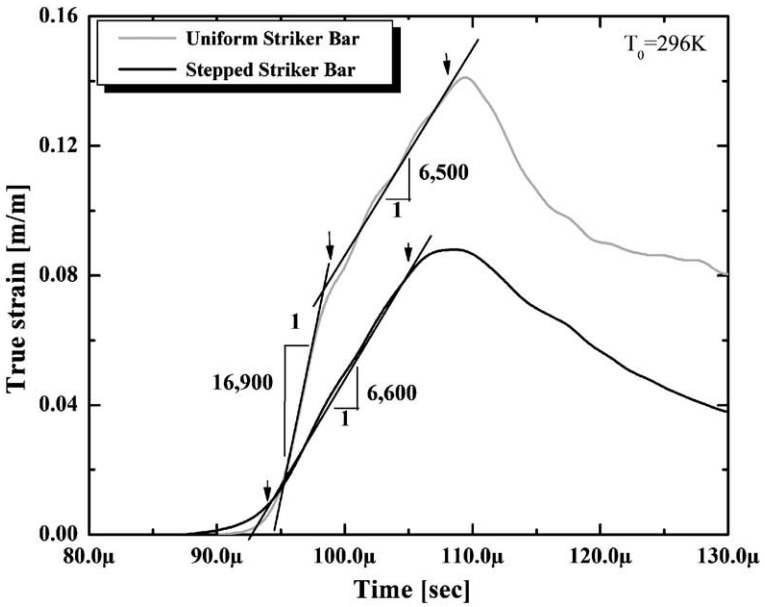

Fig. 7. Strain as a function of time obtained using mini-Hopkinson bar with uniform and stepped striker bars.

3.3. Strain-rate sensitivity of NiTi

At a temperature below M_d, which is the maximum temperature for the stress-induced martensite formation, the stress–strain curve of this material exhibits two transition stresses, depending on the strain range. One is the transition stress for the stress-induced martensite formation, and the other is the yield stress of the resulting martensite. Fig. 8 shows the variation of the stress for the stress-induced martensite formation and the yield stress of the resulting material, with the strain rate.

First, we consider the strain-rate sensitivity of the transition stress for the stress-induced martensite formation, including the results by Nemat-Nasser et al. (in press). As mentioned before, we calculate the strain rate at strains below 0.06 in the case of the 1/2-in. Hopkinson bar tests. From the mini-Hopkinson bar tests, we only include the results obtained using the stepped striker bars. We use the inflection point on the stress–strain curve obtained by the mini-Hopkinson bar, as the transition stress for the stress-induced martensite formation. The transition stress increases gradually with the increasing strain rate until about 1000/s, and then it increases rapidly with the increase in the strain rate above 1000/s. The transition stress doubles from approximately 300 to 600 MPa, as the strain rate increases from 10^{-4}/s to approximately 5000/s, whereas it increases by the same 300 MPa when the strain rate increases from 5000 to 6600/s.

According to a model proposed by Olson and Cohen (1979) for the nucleation and growth of martensites, the interface between the austenite and martensite phases consists of coherency dislocations or misfit dislocations. Thus, interfacial motion is of fundamental importance in the nucleation and growth of the martensite phase. On the basis of the dislocation model of the interfacial structure, the strain-rate dependence of the motion of the interface is expected to be similar to that of slip dislocations. Grujicic et al. (1982, 1985) studied the kinetics of the interfacial motion in a thermoelastic Cu–Al–Ni alloy and proposed a thermally activated interfacial motion model for the interface velocity. They also mentioned that the mobility of twinned martensites is greater than that of the dislocation martensites, due to the weak interaction of the twinned interface with various obstacles. This thermally activated interfacial motion model does explain the dependence of the

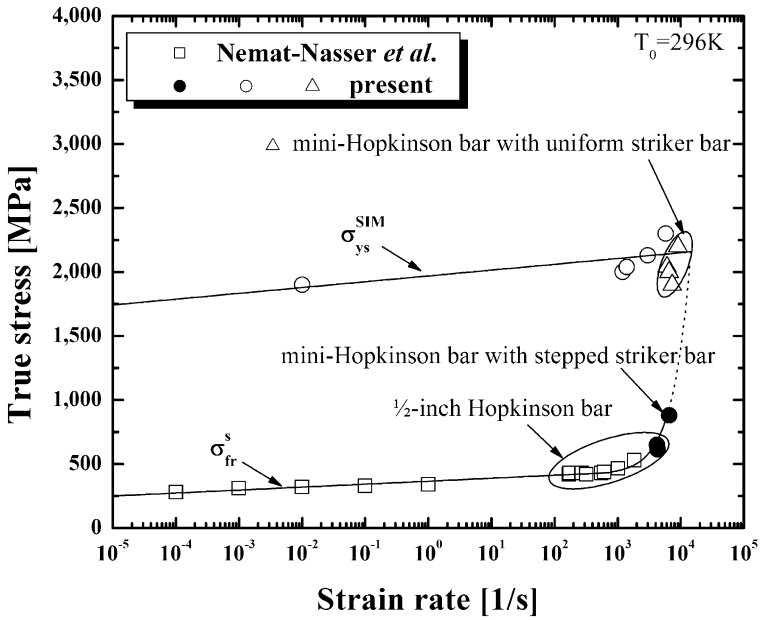

Fig. 8. Transition stress of stress-induced martensite formation and the yield stress of the resulting martensites as functions of strain rate; the triangles denote the yield stress of parent austen obtained from Fig. 6.

stress on the strain rate, at strain rates below around 1000/s, but it does not seem to explain the rapid increase of the stress at strain rates around 1000/s. At strain rates above 1000/s, there may be an additional resistance due to the interfacial drag effect, similar to that which affects the dislocation-slip motion at high strain rates (Kapoor and Nemat-Nasser, 2000).

We now examine the effect of the strain rate on the yield stress of the resulting stress-induced martensite phase. As is shown in Fig. 8, this yield stress in a quasi-static test is lower than that obtained in the 1/2-in. Hopkinson bar test, indicating that the yield stress of the resulting martensite increases with the increase in the strain rate. However, even though both strain rates in the 1/2-in. and the mini-Hopkinson bars are similar within the plastic deformation range, the yield stress of the material measured in the 1/2-in. Hopkinson bar is higher than that measured in the mini-Hopkinson bar. As seen in Fig. 7, the strain rate attained in the mini-Hopkinson bar within the superelastic range is about 4 times greater than that attained in the 1/2-in. Hopkinson bar, affecting differently the subsequent yielding response of the material. This huge difference in the strain rate within the superelastic range, strongly affects the plastic yielding behavior of the material, likely due to its effect on the phase transformation mechanism. This is verified by microstructural observation, using TEM.

Fig. 9 displays the microstructure of a specimen that has been plastically deformed at a strain rate of 10^{-2}/s in a quasi-static test. In Fig. 9(a), the stress-induced martensite variant has an internally twinned structure, with the remaining areas indicating the occurrence of a detwinning process in the stress-induced martensite variants. The bright field image in Fig. 9(b) and the dark field image in Fig. 9(c), obtained at the spot indicated by a white arrow in Fig. 9(d), clearly show that the variant of the stress-induced martensite is formed by a mechanical twinning process, with some variants having undergone a detwinning process (indicated by a single arrow in Fig. 9(c)). Especially the twinned interfaces in the plastically deformed stress-induced martensite in Fig. 9(c), are seen as straight lines (a double arrow).

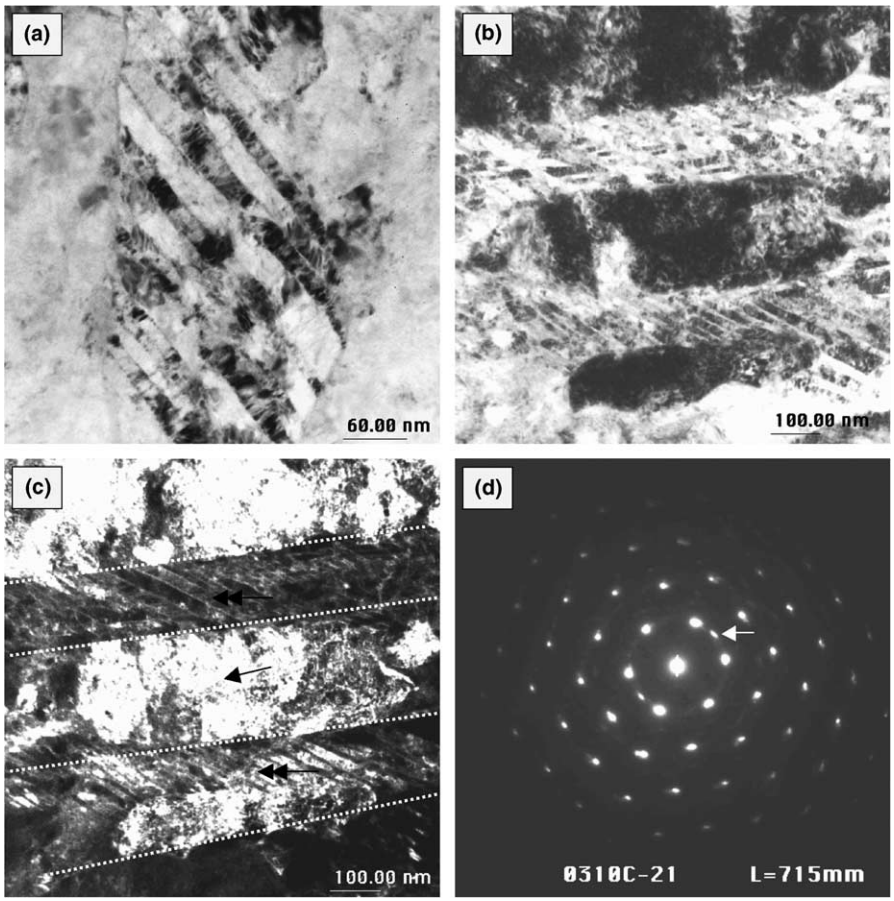

Fig. 9. TEM micrographs of a plastically deformed NiTi specimen with a residual strain of 0.15, tested quasi-statically: (a) bright field image at low magnification, (b) bright field, and (c) dark field of (b) at the indicated spot on the diffraction pattern in (d).

Fig. 10 shows TEM micrographs of a plastically deformed specimen with a residual strain of about 0.16, deformed at a strain rate of 3000/s, using a 1/2-in. Hopkinson bar. The TEM microstructure of this specimen shows a banded structure which is produced by the plastic deformation of the resulting stress-induced martensite variants, being essentially the same as that in Fig. 9 for the quasi-static test. The white dotted lines in Fig. 10(a) indicate the resulting stress-induced martensite variants, consisting of the twins with curved interfaces. Fig. 10(b) shows that the detwinning process has occurred in some (indicated by a single arrow), but not in all variants. The distinct feature produced by a moderately high strain-rate deformation is the curved interface of the resulting twin and variant martensites, whereas those in the quasi-static cases are essentially flat. These observations suggest that, at moderately high strain rates below a certain critical value, first the stress-induced martensites are formed and then they are plastically deformed. Thus, the yield stress represents the plastic deformation of the resulting stress-induced martensites.

Fig. 11 exhibits TEM micrographs of a plastically deformed specimen with a residual strain of about 0.08, tested at strain rates which exceeded 10,000/s over the superelastic deformation range, using a mini-Hopkinson bar. As mentioned before, the average strain rate attained in the mini-Hopkinson bar test, for strains below 0.08, is approximately 16,900/s, whereas that for strains above

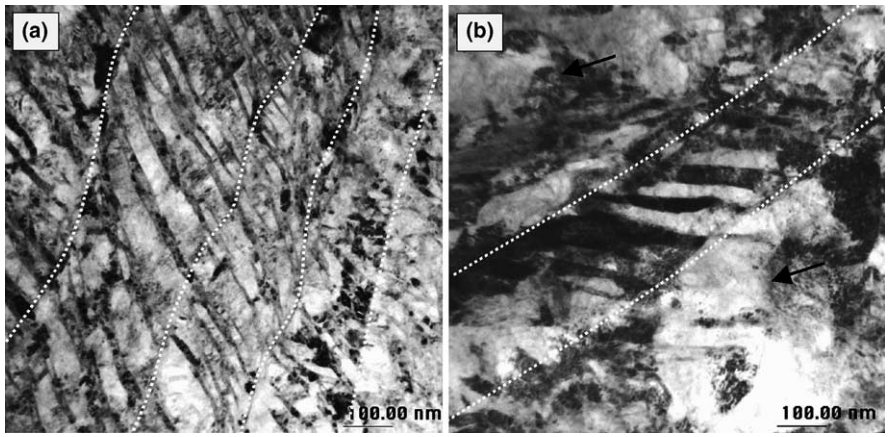

Fig. 10. TEM micrographs of a plastically deformed NiTi specimen with a residual strain of 0.16, tested in the 1/2-in. Hopkinson bar.

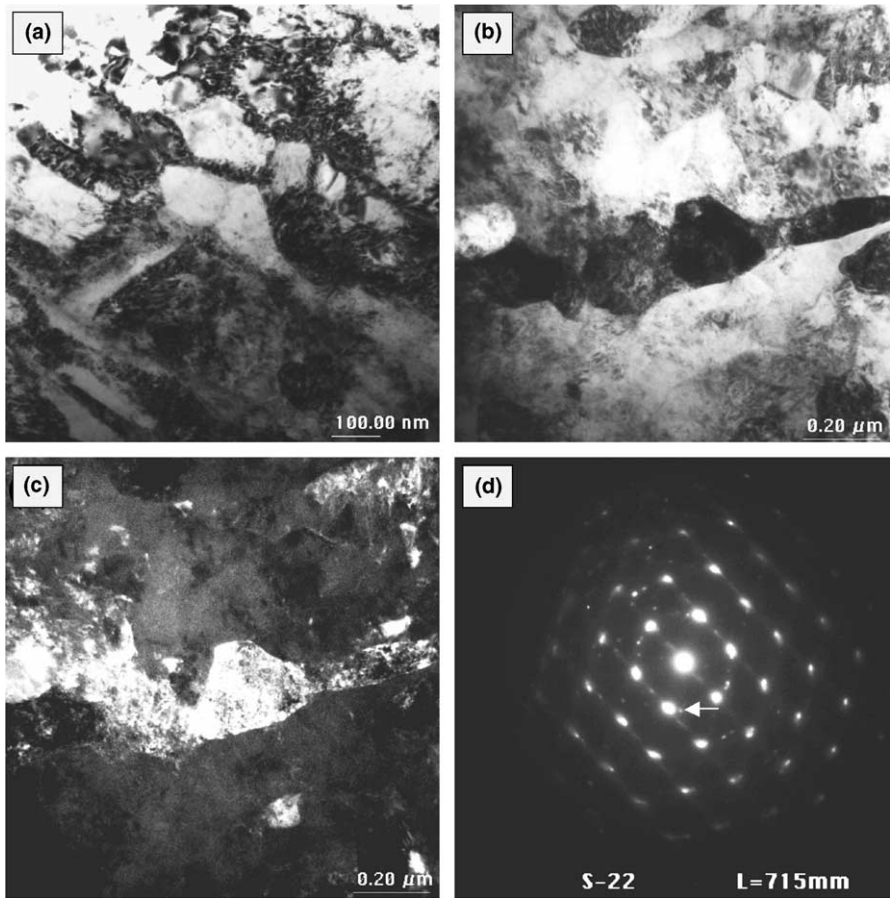

Fig. 11. TEM micrographs of a plastically deformed NiTi specimen with a residual strain of 0.08, tested in the mini-Hopkinson bar: (a) bright field image of dislocation structure, (b) bright field image of dislocation structure, and (c) dark field image of (b) at the spot indicated on the diffraction pattern of (d).

0.08 is approximately 6500/s (the open triangles in Fig. 8). The TEM microstructure of the deformed specimen does not show any stress-induced martensites. As shown in Fig. 11(a) and (b), the plastic deformation occurs by the dislocation-induced slip, forming dislocation cells in the austenite phase, and this is confirmed by the diffraction pattern shown in Fig. 11(d). These different microstructures can explain the different yield stresses measured for the same initial material, using the 1/2-in. and the mini-Hopkinson bars. Due to the very high strain rate attained during the stress-induced martensite formation, the stress level required for the stress-induced martensite formation is higher than that required to deform the austenite phase plastically. At such a strain rate, the deformation occurs by dislocation slip of austenites, as in an ordinary metal. Results in Figs. 8–11 suggest that there exists a critical strain rate, above which no stress-induced martensites are formed. At a strain rate below this critical level, the stress-induced martensites are formed within the superelastic strain range, and, then, further loading plastically deforms the resulting martensites, whereas no martensites are formed at a strain rate above this critical value, the deformation of the parent austenites then occurs by a dislocation-induced plastic slip.

4. Conclusions

In summary, compressive tests are performed on cylindrical samples to investigate the mechanical response of a NiTi shape-memory alloy at various strain rates, using UCSD's modified split Hopkinson bar and a mini-Hopkinson bar. Several noteworthy conclusions are as follows:

1. A relatively constant strain rate is attained during the formation and plastic deformation of the stress-induced martensite phase, using a 1/2-in. Hopkinson bar with a pulse-shaping technique, and for very high strain rates, using a mini-Hopkinson bar with stepped striker bars.
2. At a very high strain rate, the stress–strain relation differs from that at a moderately high strain rate, suggesting that different material responses may be involved in the corresponding phase transition regimes.
3. The stress for the austenite to martensite phase transition, shows a sudden increase at strain rates around 1000/s. This strain-rate sensitivity can be explained by considering the interfacial motion of the formed martensite, based on a model that includes the thermal activation and the dislocation drag effects.
4. The yield stress of the martensite phase appears to be strain-rate dependent in the range of the strain rates attained using a 1/2-in. Hopkinson bar. However, at greater strain rates attained using a mini-Hopkinson bar, a different deformation mechanism must become operative, basically due to the effect of very high strain rates on the deformation within the superelastic strain range.
5. The deformation of the material at very high strain rates, e.g., 17,000/s, occurs by the direct dislocation-induced plastic slip of the parent austenite phase, as is confirmed through TEM microstructural observation that shows the resulting dislocation cell structure.
6. A certain critical strain rate exists, at which the transition stress for the stress-induced martensite formation equals the yield stress of the parent austenite phase. At strain rates lower than this critical value, the shape-memory alloy deforms by the formation of the stress-induced martensites, followed by the plastic yielding of the resulting martensites, while it deforms by the dislocation-induced plastic slip of the austenite phase, at strain rates above this critical value.

Acknowledgments

This work was supported by ONR (MURI) grant N000140210666 to the University of California, San Diego. The authors wish to express their appreciation to Professor M. Taya at the University of Washington for supplying the material.

References

Chen, W.W., Wu, Q., Kang, J.H., Winfree, N.A., 2001. Compressive superelastic behavior of a NiTi shape memory

alloy at strain rates of 0.001–750 s^{-1}. Int. J. Solids Struct. 38, 8989–8998.

Entemeyer, D., Patoor, E., Eberhardt, A., Berveiller, M., 2000. Strain rate sensitivity in superelasticity. Int. J. Plasticity 16, 1269–1288.

Grujicic, M., Olson, G.B., Owen, W.S., 1982. Kinetics of martensitic interface motion. J. Phys. C 4, 173–178.

Grujicic, M., Olson, G.B., Owen, W.S., 1985. Mobility of martensitic interfaces. Metall. Trans. A 16, 1713–1722.

Jacobus, K., Sehitoglu, H., Balzer, M., 1996. Effect of stress state on the stress-induced martensitic transformation in polycrystalline Ni–Ti alloy. Metall. Trans. A 27, 3066–3073.

Kapoor, R., Nemat-Nasser, S., 2000. Comparison between high and low strain-rate deformation of tantalum. Metall. Mater. Trans. A 31, 815–823.

Lin, P.-H., Tobushi, H., Tanaka, K., Hattori, T., Ikai, A., 1996. Influence of strain rate on deformation properties of TiNi shape memory alloy. JSME Int. J. A 39, 117–123.

McCormick, P.G., Liu, Y., Miyazaki, S., 1993. Intrinsic thermal–mechanical behavior associated with the stress-induced martensitic transformation in NiTi. Mater. Sci. Eng. A 167, 51–56.

Nemat-Nasser, S., Choi, J.Y., Guo, W.-G., Isaacs, J.B., Taya, M., in press. High strain-rate, small strain response of a NiTi shape-memory alloy. J. Eng. Mater. Technol.

Nemat-Nasser, S., Isaacs, J.B., 1997. Direct measurement of isothermal flow stress of metals at elevated temperatures and high strain rates with application to Ta and Ta–W alloys. Acta Mater. 45, 907–919.

Nemat-Nasser, S., Isaacs, J.B., Starrett, J.E., 1991. Hopkinson techniques for dynamic recovery experiments. Proc. Roy. Soc. Lond. A 435, 371–391.

Olson, G.B., Cohen, M., 1979. Interface-boundary dislocations and the concept of coherency. Acta Metall. 27, 1907–1918.

Otsuka, K., Wayman, C.M., 1998. Shape Memory Materials. Cambridge University Press, Cambridge.

Shaw, J.A., Kyriakides, S., 1995. Thermomechanical aspects of NiTi. J. Mech. Phys. Solids 43, 1243–1281.

Shaw, J.A., Kyriakides, S., 1997. On the nucleation and propagation of phase transformation fronts in a NiTi alloy. Acta Mater. 45, 683–700.

Tobushi, H., Takata, K., Shimeno, Y., Nowacki, W.K., Gadaj, S.P., 1999. Influence of strain rate on superelastic behavior of TiNi Shape memory alloy. Proc. Inst. Mech. Eng. 213 (part L), 93–102.

Van Humbeeck, J., 1999. Non-medical applications of shape memory alloys. Mater. Sci. Eng. A 237–275, 134–148.

Van Humbeeck, J., 2001. Shape memory alloys: a material and a technology. Adv. Eng. Mater. 3, 143–156.